Signal Interception: A Unifying Theoretical Framework for Feature Detection

WILLIAM A. GARDNER, SENIOR MEMBER, IEEE

Abstract—**The unifying framework of the spectral correlation theory of cyclostationary signals is used to present a broad treatment of weak random signal detection for interception purposes. The relationships among a variety of previously proposed ad hoc detectors, optimum detectors, and newly proposed detectors are established. The spectral-correlation-plane approach to the interception problem is put forth as especially promising for detection, classification, and estimation in particularly difficult environments involving unknown and changing noise levels and interference activity. A fundamental drawback of the popular radiometric methods in such environments is explained.**

I. INTRODUCTION

INTERCEPTION of communications is attempted for a variety of reasons including reconnaissance, surveillance, and other intelligence gathering activities, as well as position fixing, identification, and communications jamming. For example, an aircraft might attempt to intercept the communications between a submarine or ship and a satellite, or a satellite might attempt to intercept ground-to-ground communications. Typically, the interceptor has knowledge of no more than the communicator's frequency band, modulation format, and modulation characteristics such as bandwidth and hop rate or chip rate. In the past, it was commonly held that the most appropriate approaches to the detection task for signal interception must be based on radiometry, that is, measurement of received energy in selected time and frequency intervals (cf. [1]–[5]). However, it is commonly recognized that such radiometric methods can be highly susceptible to unknown and changing noise levels and interference activity. There have been many proposals for methods of countering such complications, including various approaches to adjusting or adapting threshold levels, and adaptive filtering, cancelling, and directional nulling of interfering signals. But these problems remain as the most serious impediment to signal detection and other signal interception tasks (cf. [4]–[6]).

The radiometric approach to detection is based on the use of stationary random processes as models for the signals to be intercepted. However, it is shown in this paper that for the purposes of signal interception, the signal of interest is more appropriately modeled as a *cyclostationary* random process, that is, a random process whose probabilistic or statistical parameters vary periodically with time [7]. The message contained in the modulated signal is unknown, and is usually modeled as a stationary random process (discrete time or continuous time). This stationarity coupled with the periodicity of sine wave carriers, pulse trains, repeating spreading codes, etc., results in a cyclostationary model for the signal. However, these cyclostationary signals typically do not exhibit spectral lines because the spectral lines of the unmodulated carriers and/or pulse trains are spread out over relatively broad bands by the stationary random modulation.

The purpose of this paper is to use the unifying framework of the spectral correlation theory of cyclostationary signals to present a broad treatment of weak random signal detection that clearly reveals the relationships among the variety of detectors that have been proposed, or are in the development stage, or are in use, and to present several arguments with supporting results that favor *cyclic-feature* detection over energy detection for accommodating the problems associated with unknown and changing noise levels and interference activity. Cyclic features result from the characteristic property of cyclostationarity called *regenerative periodicity,* which means that spectral lines can be regenerated from the signal with the use of appropriate nonlinear transformations [8].

Before proceeding to the technical part of this paper, let us consider the signal interception problem and the strengths and weaknesses of radiometry and cyclic-feature detection in a little more detail.

A. Drawbacks of Radiometry

The communication bands below 3 GHz have grown increasingly dense with both military and commercial communication systems in the last decade. This creates an especially severe environment for distinguishing signals of interest from background noise and interfering signals. In airborne reconnaisance systems, for instance, where the collection area can contain hundreds of emitters, this is particularly problematic. In addition, there is a clear trend towards increased use of systems employing sophisticated signal formats such as direct-sequence and frequency-hopped spread-spectrum modulation, both to aid communication in this environment and to protect the communication system against interception. In these applications, it is unlikely that conventional radiometry will be able to perform required signal detection or subsequent analysis tasks. The complex collection environment is likely to overwhelm the signals of interest, since they can be buried beneath much stronger groupings of interfering signals. In addition, the modulation format of the signal of interest can make it indistinguishable from the noise background. This can occur, for example, if the signal is direct-sequence spread-spectrum modulated with no easily identifiable spectral features to distinguish it from other signals. In code-division and frequency-hop multiple access systems, the signals of interest even interfere with each other. The presence of several identically distributed spectrally superimposed signals will confuse most energy detection schemes, preventing the interceptor from determining any more than knowledge that signals are present in the environment. Furthermore, radiometry suffers from inherent limitations that prevent if from being used for some signal analysis applications. In particular, energy detection schemes are

Paper approved by the Editor for Communication Theory of the IEEE Communications Society. Manuscript received August 15, 1986; revised March 20, 1987. This work was supported by the Naval Postgraduate School. This paper was presented at the Eleventh GRETSI Symposium on Signal and Image Processing, Nice, France, June 1–5, 1987, and is based on "Spread Spectrum Detection: A Unifying View," Signal and Image Processing Laboratory Technical Report SIPL-85-6, Department of Electrical Engineering and Computer Science, University of California, Davis, CA, January 1985.

The author is with the Signal and Image Processing Laboratory, Department of Electrical Engineering and Computer Science, University of California, Davis, CA 95616.

IEEE Log Number 8822461.

0090-6778/88/0800-0897$01.00

inherently unable to measure or exploit timing or phasing properties (carrier phase, chip, or baud timing) of the signals of interest or interferences because these energy detectors usually cannot exploit the cyclostationary, or periodically time-variant, signal characteristics. In practice, collection systems overcome this restriction by such means as 1) analyzing successions of short-collect power spectra to exploit gross signal timing, such as time-of-arrival or slow hop rate of signals of interest, 2) using multisensor techniques to exploit spatial distribution of the energy of signals of interest and interferences [9], or 3) completely abandoning energy detection techniques for schemes that exploit the modulation characteristics of the signal of interest and/or interferences, such as baud, chip, or hop rate[1] [10]. These latter schemes, often referred to as *cyclic-feature detection* techniques, have many advantages over radiometry, including the ability to perform signal timing measurement, discriminate against signals not of interest using sufficiently long collects, and reduce sensitivity to unknown and changing background noise level and interference activity. These techniques can be thought of as ad hoc realizations of a generalization of energy detection and power spectral analysis, referred to here as *spectral correlation detection* or *cyclic spectral analysis* [8].

B. Advantages of Cyclic-Feature Detection

There are three important advantages of cyclic spectral analysis over energy detection techniques, the first of which is its discriminatory capability. Signal features are discretely distributed in cycle frequency in the cyclic spectrum, even if the signal has continuous distribution in the power spectrum. Thus, signals with overlapping features in the power spectrum can have nonoverlapping features in the cyclic spectrum. Background noise, for instance, has no features at nonzero cycle frequencies; analyzing the cyclic spectrum at a nonzero cycle frequency where a signal-of-interest feature is expected to appear will reveal that feature without any component due to the background noise (except measurement noise which can be substantial, but which decreases with increasing collect). A theoretical analysis of the signals of interest and interferences can reveal regions of the cyclic spectrum where signal-of-interest features will appear, but interference features will not. TV signals, for instance, have primary features at cycle frequencies that are multiples of the TV-signal horizontal line-scan rate (15.75 kHz in the USA, 15.625 kHz in Europe and the USSR); if the signal-of-interest has features at other cycle frequencies, then analysis of the cyclic spectrum at those cycle frequencies will reveal those features without any component due to the interference (again, except measurement noise). The JAGUAR V signal [11], for example, has cyclic spectral features at the 100 Hz hop rate, and also at the 19.2 kHz FSK baud rate; analysis of the cyclic spectrum at multiplies of 100 Hz or 19.2 kHz in cycle frequency will reveal JAGUAR V features even in the presence of significant TV interference. Signals can also be separated by Doppler shift in the cyclic spectrum, a capability that is not available with the power spectrum.

To illustrate this discriminatory capability of cyclic spectral analysis, the measured cyclic spectrum magnitude is graphed in Fig. 1(a) as the height of a surface above a plane with coordinates of frequency f and cycle frequency α. This cyclic spectrum was computed using the frequency-smoothed cyclic

[1] Pioneering work on ad hoc cyclic-feature detectors carried out in the mid-to-late 1970's is reported in the unpublished document [10]. Much work on evaluating the utility of specific ad hoc cyclic-feature detectors (chip-rate and hop-rate detectors, and carrier doublers and quadruplers) has been done since that time, most of which has not been published, although a few papers have been presented at the MILCOM conferences. A general approach to optimal detection of digitally modulated signals based on the maximum-likelihood criterion, which leads to multicycle feature detectors, as defined in the present paper, is reported in [21].

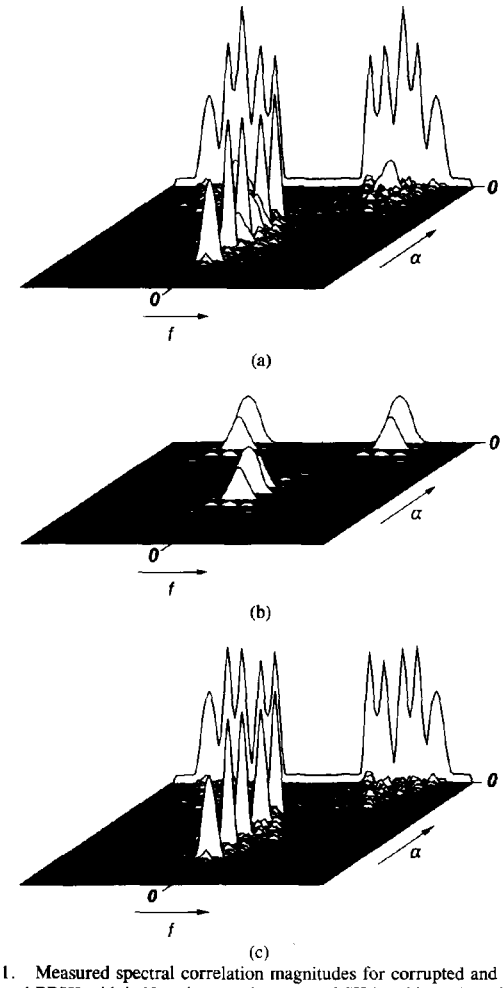

Fig. 1. Measured spectral correlation magnitudes for corrupted and uncorrupted BPSK with half-cosine envelope. (a) BPSK in white noise with five AM interferences. (b) Uncorrupted BPSK. (c) White noise and AM interferences only.

periodogram

$$S^{\alpha}_{x_T}(f)_{\Delta f} \triangleq \frac{1}{M+1} \sum_{m=-M/2}^{M/2} S^{\alpha}_{x_T}(f+m/NT_s)$$

where

$$S^{\alpha}_{x_T}(f) \triangleq \frac{1}{N} X_T(f+\alpha/2) X^*_T(f-\alpha/2)$$

$$X_T(f) \triangleq \sum_{n=0}^{N-1} x(nT_s) e^{-i2\pi nm/NT_s},$$

and where $T = NT_s$ is the segment length and $\Delta f = (M + 1)/NT_s$ is the frequency-smoothing window width. The parameters used are $N = 32\,768$ and $M = 1024$. The data $x(nT_s)$ consist of a BPSK signal of interest with a half-cosine envelope and a bandwidth of BW $= 0.1875/T_s$, five interfering AM signals with bandwidths ranging from BW $= 0.04/T_s$ to BW $= 0.08/T_s$, and white noise. The SNR is 0 dB and the SIR for each interference is 0 dB. Thus, the total SINR is -8 dB. In Fig. 1(b), the measured cyclic spectrum magnitude for the BPSK signal alone is shown and in Fig. 1(c)

the measurement for the interference and noise alone is shown. The $\alpha = 0$ part of these graphs represents the measured power spectral density. It can be seen by comparing Fig. 1(a)–(c) that the BPSK signal is completely masked in the power spectral density measurement ($\alpha = 0$) but is clearly revealed in the cyclic spectral density measurement ($\alpha \neq 0$). These results would be even more striking with FM interference because the $\alpha \neq 0$ features for commonly occurring FM interference (e.g., push-to-talk FM) are very small compared to the $\alpha \neq 0$ features shown here for AM.

The second advantage of cyclic spectral analysis is that the cyclic spectrum is a much richer domain for signal analysis than the conventional power spectrum. In addition to the signal separation provided by the cyclic spectrum magnitude, sine-wave-carrier and pulse-train frequency and phase parameters can also be measured from the cyclic spectrum magnitude and phase [12], [13]. This allows cyclic spectral analysis to be used as a much more complete tool for signal analysis, compared to the power spectrum; it also opens the door to new ways to separate signals on the basis of timing and phasing as well as cycle frequency. In some applications, such as radio communication networks where many identically distributed signals of interest can be superimposed even in the cyclic spectrum, this capability might prove to be crucial.

The third advantage of cyclic spectral analysis lies in the theory underlying the techniques. The cyclic spectrum, which is composed of spectral correlation functions, provides a much more complete mechanism for modeling communication signals than the power spectrum; the mathematics needed to perform this modeling, however, are not significantly more complex [7]–[8], [14]–[16]. It is shown in this paper that both conventional spectrum analyzers and feature detection techniques can be theoretically studied and analyzed in terms of the cyclic spectrum. It is also shown that, in addition to ad hoc feature detection and nonparametric approaches (power spectral analysis and cyclic spectral analysis) to detecting and analyzing signals, optimal parametric approaches that can be implemented in terms of cyclic spectral analysis can also be devised.

The focus in this paper is on interpreting the various detector structures within the unifying conceptual framework of spectral correlation. A sequel to this paper will employ this unification to carry out performance analysis that supports the claim that cyclic-feature detection has the potential for outperforming radiometry for interception in problematic noise and interference environments. But even without such analyses, graphs such as those in Fig. 1 strongly suggest that this claim can be supported. One example is briefly considered at the end of this paper to demonstrate the superiority of cyclic-feature detectors.

II. Spectral Correlation

For the purposes of signal interception, the signal of interest is most appropriately modeled as a *cyclostationary* random process, whose probabilistic or statistical parameters vary periodically with time, reflecting the characteristic property of regenerative periodicity. If there is more than one source of periodicity and the periods are not all commensurate, then the process is called *almost cyclostationary* since its parameters are almost periodic functions of time (that is, sums of periodic functions with incommensurate periods). For example, the autocorrelation function

$$R_x(t+\tau/2,\ t-\tau/2) = E\{x(t+\tau/2)x(t-\tau/2)\} \tag{1}$$

for the signal $x(t)$, by virtue of the (almost) cyclostationarity of $x(t)$, will be a (almost) periodic function of the variable t, and will therefore admit the Fourier series representation

$$R_x(t+\tau/2,\ t-\tau/2) = \sum_{\alpha} R_x^{\alpha}(\tau) e^{i2\pi\alpha t} \tag{2}$$

where the sum is over integer multiples of fundamental frequencies (reciprocals of periods), such as carrier frequency, baud rate, chip rate, hop rate, and their sums and differences. The Fourier coefficients $R_x^{\alpha}(\tau)$, which depend on the lag parameter τ, are given by the formula

$$R_x^{\alpha}(\tau) = \lim_{Z\to\infty} \frac{1}{Z} \int_{-Z/2}^{Z/2} R_x(t+\tau/2,\ t-\tau/2) e^{-i2\pi\alpha t}\, dt. \tag{3}$$

(If there is only one period, say T, then Z can be chosen equal to T, and the limit in (3) can be omitted.) If $x(t)$ is a *cycloergodic* process [7], [17] (which it always will be if an appropriate model is used), then after substitution of (1) into (3), the expectation operator can be omitted to obtain

$$R_x^{\alpha}(\tau) = \lim_{Z\to\infty} \frac{1}{Z} \int_{-Z/2}^{Z/2} x(t+\tau/2)x(t-\tau/2) e^{-i2\pi\alpha t}\, dt. \tag{4}$$

(When (4) is used in place of (3), the limit $Z \to \infty$ cannot be omitted when there is only one period.) The function $R_x^{\alpha}(\tau)$ is called the *cyclic autocorrelation function*. For $\alpha = 0$, it reduces to the conventional autocorrelation function $R_x^0(\tau)$. Whereas $R_x^0(\tau)$ can be seen from (4) to be the dc component of the lag-product waveform $x(t + \tau/2)x(t - \tau/2)$ for each value of τ, $R_x^{\alpha}(\tau)$ can be seen to be the ac component corresponding to sine-wave frequency α.

The Fourier transform

$$S_x^{\alpha}(f) = \int_{-\infty}^{\infty} R_x^{\alpha}(\tau) e^{-i2\pi f\tau}\, d\tau \tag{5}$$

is called the *cyclic spectral density function*. For $\alpha = 0$ it reduces to the conventional power spectral density function, that is, the spectral density of time-averaged power. However, for $\alpha \neq 0$, it can be shown that $S_x^{\alpha}(f)$ is the density of spectral correlation, that is, the density of correlation between spectral components at the frequencies $f + \alpha/2$ and $f - \alpha/2$. Specifically, it is shown in [7], [8], [14], [15] that

$$S_x^{\alpha}(f) = \lim_{T\to\infty} \lim_{Z\to\infty} \frac{1}{TZ} \int_{-Z/2}^{Z/2} X_T(t, f+\alpha/2) \cdot X_T^*(t, f-\alpha/2)\, dt \tag{6}$$

where $X_T(t, f)$ is the complex envelope of the narrowband spectral component with center frequency f and bandwidth on the order of $1/T$,

$$X_T(t, f) = \int_{t-T/2}^{t+T/2} x(u) e^{-i2\pi f u}\, du. \tag{7}$$

Thus, $S_x^{\alpha}(f)$ is also called the *spectral correlation function*, and it follows from the preceding discussion that spectral correlation is a characteristic property of cyclostationarity of the autocorrelation.

The most common approach to modeling signals for interception studies (cf. [4], [5]) is to ignore cyclostationarity by either 1) introducing a random phase variable θ uniformly distributed over one period of the cyclostationarity (or a sum of such phases, one for each period of an almost cyclostationary process) so that $x(t + \theta)$ becomes stationary [7], [18]—that is, only the $\alpha = 0$ term in (2) is then nonzero—or 2) using the time-average approach based on (4), and simply ignoring the $\alpha \neq 0$ averages. This approach is appropriate if there is no desire to exploit cyclostationarity, and it leads to the popular conclusion that the radiometer is essentially the optimum detector (cf. [7].) Therefore, the adoption in this paper of the cyclostationary model marks the point of departure of this work from many previous studies of signal interception. Nevertheless, since the stationary model is a

special case of the cyclostationary model, the results derived in this paper include the more conventional results as special cases.

Example: Consider the noise-free AM signal $x(t) = s(t)$,

$$s(t) = a(t) \cos (2\pi f_c t + \phi_0) \tag{8}$$

where $a(t)$ is a stationary process. It is easily shown using (4) that

$$R_s^\alpha(\tau) = \begin{cases} \frac{1}{2} R_a^0(\tau) \cos (2\pi f_c \tau), & \alpha = 0 \\ \frac{1}{4} R_a^0(\tau) e^{\pm i2\phi_0}, & \alpha = \pm 2f_c, \end{cases} \tag{9}$$

and $R_s^\alpha(\tau) = 0$ for all other values of α. Or using (1), we obtain

$$R_s(t+\tau/2, t-\tau/2) = \frac{1}{2} R_a^0(\tau) [\cos (2\pi f_c \tau) + \cos (4\pi f_c t + 2\phi_0)], \tag{10}$$

from which (9) follows using (3). Fourier transformation of (9) yields

$$S_s^\alpha(f) = \begin{cases} \frac{1}{4} [S_a^0(f-f_c) + S_a^0(f+f_c)], & \alpha = 0 \\ \frac{1}{4} S_a^0(f) e^{\pm i2\phi_0}, & \alpha = \pm 2f_c. \end{cases} \tag{11}$$

Thus, the only spectral components that are correlated are those whose frequencies are separated by $|\alpha| = 2f_c$. This is easy to see intuitively since multiplication of $a(t)$ by $\cos (2\pi f_c t + \phi_0)$ as in (8) shifts each spectral component in $a(t)$ up and down by the amount f_c. Thus, the spectral components at $f + f_c$ and $f - f_c$ in $s(t)$ are one and the same as the spectral component at f in $a(t)$. So they are obviously correlated.

Explicit formulas for the spectral correlation function have recently been calculated for the majority of types of modulated signals used in modern communication systems in [7], [8], [15], [16]. A variety of analog and digital methods for measurement of spectral correlation have been described in [8], [12].

III. Detection by Spectral-Line Regeneration

Perhaps the most straightforward interpretation of most cyclic-feature detectors is that they use a nonlinearity to regenerate a spectral line from the noisy modulated signal, and then use a bandpass filter, DFT, or other methods of spectral analysis to detect the presence of the regenerated spectral line which is masked by continuous spectral components due to noise, interference, and the signal of interest itself. Since the signal-to-noise ratio (SNR) is often very low in an interception environment, the lowest order nonlinearity is usually chosen since an SNR of less than 0 dB becomes increasingly lower as the order of the nonlinearity used is increased. Thus, most feature detectors use quadratic nonlinearities. (An exception is carrier regeneration for balanced QAM signals, such as QPSK, since these require higher order nonlinearities for spectral-line regeneration [19].) Hence, most feature detectors are quadratic time-invariant systems which can always be represented by

$$y_\alpha(t) = \int_{-\infty}^{\infty} \int_{-\infty}^{\infty} k_\alpha(u, v) x(t-u) x(t-v)\, du\, dv \tag{12}$$

where α represents the frequency of the spectral line to be regenerated from $x(t)$. For example, the delay-and-multiply chip-rate-feature detector (cf. [10], [20]) can be expressed as

$$y_\alpha(t) = \{h(t) \otimes x(t)[h(t-\tau_o) \otimes x(t-\tau_o)]\} \otimes g(t) \tag{13}$$

where $h(t)$ is the impulse-response function of a prefilter, τ_o is the delay (typically chosen to be half the chip interval), and $g(t)$ is the impulse response of a postfilter (e.g., a bandpass filter with center frequency α). Equation (13), in which $\otimes$ denotes convolution, can be put into the form of (12) with kernel

$$k_\alpha(u, v) = \int_{-\infty}^{\infty} h(u-w) h(v-w-\tau_o) g(w)\, dw. \tag{14}$$

Similarly, for the filter-squarer carrier-feature detector, we have

$$y_\alpha(t) = [h(t) \otimes x(t)]^2 \otimes g(t) \tag{15}$$

which is simply (13) with $\tau_o = 0$. Thus, (15) can be put into the form of (12) with kernel

$$k_\alpha(u, v) = \int_{-\infty}^{\infty} h(u-w) h(v-w) g(w)\, dw. \tag{16}$$

Also, for the dual-channel correlation detector, we have

$$y_\alpha(t) = \{h_1(t) \otimes x(t)[h_2(t) \otimes x(t)]\} \otimes g(t) \tag{17}$$

where $h_1(t)$ and $h_2(t)$ are the impulse-response functions of bandpass filters with center frequencies f_1 and f_2, and $g(t)$ is the impulse-response function of a bandpass filter with center frequency $\alpha = |f_1 - f_2|$. Equation (17) can be put into the form of (12) with kernel

$$k_\alpha(u, v) = \int_{-\infty}^{\infty} h_1(u-w) h_2(v-w) g(w)\, dw. \tag{18}$$

The approach in the past has been to choose the particular detector structure, such as (13), (15), or (17), and then to optimize its parameters, such as the delay τ_o and prefilter bandwidths. An alternative approach that puts these ad hoc detectors into better perspective is to analytically solve for the kernel $k_\alpha(u, v)$ in the general representation (12) that regenerates the strongest possible spectral line at some appropriate frequency α for a specific signal type. This same objective applies not only to the design of feature detectors for interception but also to the design of synchronizers that operate on the basis of using a phase-lock loop to lock on to the phase of a regenerated carrier or clock signal.

It has recently been shown [8], [13] that the particular kernel that maximizes the SNR of the regenerated spectral line for a cyclostationary signal $s(t)$ in additive stationary Gaussian noise and interference $n(t)$, $x(t) = s(t) + n(t)$, is specified by

$$k_\alpha(u, v) = \begin{cases} \int_{-\infty}^{\infty} \int_{-\infty}^{\infty} K_\alpha(f, v) e^{i2\pi(fu - vv)}\, df\, dv, \\ \qquad |u|, |v| \leqslant T/2, \\ 0, \qquad \text{otherwise} \end{cases} \tag{19}$$

where T is the collect time of the detector, and

$$K_\alpha(f, v) = \left[\frac{S_s^\alpha(f-\alpha/2)^*}{S_n^0(f) S_n^0(f-\alpha)} \right] \delta(f-v-\alpha), \quad \alpha \neq 0. \tag{20}$$

In the derivation of (19)–(20), it is assumed that T is large

enough that a spectral window of width $1/T$ will resolve $S_s^\alpha(f)$ and $S_n^0(f)$ (i.e., $1/T$ must be smaller than the widths of all peaks and valleys in these spectral functions). Thus, the optimum spectral line regenerator is completely specified by the spectral correlation function for the signal and the power spectral density for the noise plus interference. Furthermore, the maximized value of SNR is given by

$$\mathrm{SNR}_{\max}^{\alpha} = \frac{T}{2}\int_{-\infty}^{\infty} \frac{|S_s^\alpha(f)|^2}{S_n^0(f+\alpha/2)S_n^0(f-\alpha/2)}\,df, \quad \alpha \neq 0 \tag{21}$$

where SNR is defined to be the ratio of the power in the regenerated spectral line to the power in the band of width $1/T$ centered at frequency α, due to the output noise plus interference.

As an example, we consider white noise $n(t)$ for which $S_n^0(f) = N_0$. In this case, (19)–(20) yield

$$k_\alpha(u, v) = \frac{1}{N_o^2}[R_s^\alpha(u-v)e^{-i\pi\alpha(u+v)}]^*, \quad |u|, |v| \leqslant T/2, \tag{22}$$

which, upon substitution into (12), yields

$$y_\alpha(t) = \frac{1}{N_o^2}\int_{-T}^{T} R_s^\alpha(\tau)^* R_{x_T}^\alpha(t, \tau)\,d\tau e^{i2\pi\alpha t} \tag{23}$$

where

$$R_{x_T}^\alpha(t, \tau) \triangleq \frac{1}{T}\int_{t-(T-|\tau|)/2}^{t+(T-|\tau|)/2} x(u+\tau/2) \cdot x(u-\tau/2)e^{-i2\pi\alpha u}\,du. \tag{24}$$

The quantity $R_{x_T}^\alpha(t, \tau)$ is called the *time-variant cyclic correlogram*. For $\alpha = 0$, it reduces to the conventional time-variant correlogram [8], [22]. If T exceeds an appropriate measure of the width of the cyclic autocorrelation function $R_s^\alpha(\tau)$, then Parseval's relation for Fourier transforms can be applied to (23) to obtain the close approximation

$$y_\alpha(t) = \frac{1}{N_o^2}\int_{-\infty}^{\infty} S_s^\alpha(f)^* S_{x_T}^\alpha(t, f)\,df e^{i2\pi\alpha t}, \quad \alpha \neq 0 \tag{25}$$

where

$$S_{x_T}^\alpha(t, f) = \int_{-\infty}^{\infty} R_{x_T}^\alpha(t, \tau)e^{-i2\pi f\tau}\,d\tau. \tag{26}$$

Substitution of (24) into (26) and application of the convolution theorem for Fourier transforms yields

$$S_{x_T}^\alpha(t, f) = \frac{1}{T}X_T(t, f+\alpha/2)X_T^*(t, f-\alpha/2) \tag{27}$$

where $X_T(t, f)$ is defined by (7). The function $S_{x_T}^\alpha(t, f)$ is called the *time-variant cyclic periodogram*. For $\alpha = 0$, it reduces to the conventional time-variant periodogram [8], [22]. For the more general case of nonwhite $n(t)$ (e.g., narrow-band interference plus noise), (25) generalizes to the approximation

$$y_\alpha(t) = \int_{-\infty}^{\infty}\left[\frac{S_s^\alpha(f)^*}{S_n^0(f+\alpha/2)S_n^0(f-\alpha/2)}\right] \cdot S_{x_T}^\alpha(t, f)\,df e^{i2\pi\alpha t}. \tag{28}$$

This approximation is close if T is large enough that a spectral window of width $1/T$ will resolve $S_n^0(f)$.

In conclusion, if the noise is white, then the maximum SNR spectral-line regeneration detector measures the cyclic periodogram of the received data $x(t)$ and correlates it (over f) with the ideal cyclic spectral density (spectral correlation) function for the signal to be detected $s(t)$, as specified by (25). On the other hand, if there is strong narrow-band interference as well as white noise, then the measurement $X_T(t, f)$ is first notched by division by $S_n^0(f)$ to obtain

$$\tilde{X}_T(t, f) \triangleq \frac{X_T(t, f)}{S_n^0(f)}. \tag{29}$$

Then the cyclic periodogram is formed

$$\tilde{S}_{x_T}^\alpha(t, f) \triangleq \frac{1}{T}\tilde{X}_T(t, f+\alpha/2)\tilde{X}_T^*(t, f-\alpha/2), \tag{30}$$

and it is correlated with the ideal cyclic spectral density function for the signal

$$y_\alpha(t) = \int_{-\infty}^{\infty} S_s^\alpha(f)^* \tilde{S}_{x_T}^\alpha(t, f)\,df e^{i2\pi\alpha t}. \tag{31}$$

[As a check on (31), it is easily verified that substitution of (29) into (30) and the result into (31) yields (28).] For weak signals, $S_s^0(f) \ll S_n^0(f)$, we have $S_n^0(f) \cong S_x^0(f)$, and $S_x^0(f)$ can be measured from the received data.

For specific signal types, the general form of the optimum detector can often be reduced to more familiar forms. For example, it is shown in [13] that for PSK type signals (31) reduces to a narrow-band rejection filter for narrow-band interference removal, followed by a matched filter (with impulse-response function equal to the time-reversed carrier burst for one keying interval), followed by a squarer and a bandpass filter.[2] This reveals that the optimum prefilter for the filter-squarer detector is a matched filter, and that although the optimum delay for the delay-and-multiply detector with no prefilter is half the chip interval, the optimum prefilter is a matched filter, and when this is used the optimum delay is zero. The degradation in SNR due to use of the suboptimum ad hoc detectors instead of the optimum detector has been evaluated and will be reported in a sequel to this paper.

IV. Detection by Cyclic Spectral Analysis

Although such familiar forms as a matched filter squarer are intuitively appealing, they are not necessarily as flexible as the general form (31). For example, if the particular signal type of interest is not known sufficiently well to obtain a good approximation to the spectral correlation function $S_s^\alpha(f)$ used in (31) as a weighting function before integration over f, then it can be replaced with a simple window such as a rectangle, whose width Δf is chosen to be as large as possible without exceeding the widths of features expected to be present in $S_s^\alpha(f)$, and whose center f is a variable parameter. The resultant detection statistic is

$$\tilde{y}_\alpha(t, f) = \frac{1}{\Delta f}\int_{f-\Delta f/2}^{f+\Delta f/2} \tilde{S}_{x_T}^\alpha(t, v)\,dv. \tag{32}$$

This frequency-smoothed cyclic periodogram is a standard estimate of the ideal weighted cyclic spectral density function $S_x^\alpha(f)$. In fact, it can be shown [8], [12] that

$$\lim_{T\to\infty} \tilde{y}_\alpha(t, f) = \frac{1}{\Delta f}\int_{f-\Delta f/2}^{f+\Delta f/2} \frac{\tilde{S}_x^\alpha(v)}{S_n^0(v+\alpha/2)S_n^0(v-\alpha/2)}\,dv, \tag{33}$$

and therefore,

$$\lim_{\Delta f\to 0}\lim_{T\to\infty} \tilde{y}_\alpha(t, f) = \frac{S_x^\alpha(f)}{S_n^0(f+\alpha/2)S_n^0(f-\alpha/2)}. \tag{34}$$

[2] The same result is arrived at using a different approach in [21].

Moreover, it can be shown that the variance of $\bar{y}_\alpha(t, f)$ is inversely proportional to $T\Delta f$ [8], [12]. Furthermore, if $n(t)$ exhibits no cyclostationarity with cycle frequency α (or no spectral correlation with frequency separation α), then $S_n^\alpha(f) \equiv 0$ and therefore,

$$S_x^\alpha(f) \equiv S_s^\alpha(f). \tag{35}$$

In conclusion, if $\bar{y}_\alpha(t, f)$ were measured and graphed as a time-variant surface above the (f, α) plane, then the presence of recognizable spectral correlation features could be used to detect signals of interest and also to classify them according to modulation type.

It should be clarified that although the optimum detector (31) specifies removal of strong narrow-band interferences as the first stage of processing as in (29), this is not as crucial as it is for radiometric detection methods (assuming long collect T) because even though a number of narrow-band interferers may be spread across the band of the signal of interest, they will not necessarily give rise to a spectral correlation feature that overlaps the features from the signal of interest (although they do contribute to measurement noise and can require long collects for adequate suppression). In fact, it is unlikely that they would because this would require that the interference exhibit cyclostationarity at the same cycle frequencies as those in the signal of interest. The cyclic spectral analysis adaptation of the optimum detector, without preprocessing for interference removal as in (29) and (32), is given by

$$y_\alpha(t, f) = \frac{1}{\Delta f} \int_{f-\Delta f/2}^{f+\Delta f/2} S_{x_T}^\alpha(t, \nu)\, d\nu \tag{36}$$

where $S_{x_T}^\alpha(t, f)$ is given by (7) and (27). A variety of methods for making this measurement and close approximations to it are described in [8] and [12]. The unique spectral correlation surfaces for a wide variety of modulation types are calculated and graphed in [7], [8], [15], [16]. As one illustrative example, the magnitude surfaces for BPSK, QPSK, SQPSK, and MSK[3] are shown in Fig. 2. Observe that although the power spectral densities are identical for BPSK, QPSK, and SQPSK, their spectral correlation surfaces for $\alpha \neq 0$ are highly distinct. For example, for BPSK, there are features at $\alpha = kf_o$ and $\alpha = \pm 2f_c + kf_o$, for all integers k where f_o is the keying rate and f_c is the carrier frequency. For QPSK, there are features only at $\alpha = kf_o$ for all integers k. For SQPSK and MSK, there are features at $\alpha = kf_o$ for only even integers k, and at $\alpha = \pm 2f_c + kf_o$ for only odd integers k. For MSK, the features at $\alpha = \pm 2f_c \pm f_o$ are especially large compared to all features in BPSK, QPSK, and SQPSK. An example of a measured magnitude surface based on (36) for a BPSK signal in multiple AM interference and noise is shown in Fig. 1.

V. Ambiguity Plane and Wigner–Ville Time-Frequency Plane Methods of Detection

Having revealed the central role played by spectral correlation and cyclic spectral analysis in the spectral-line regeneration approach to detection, let us now turn to the task of interpreting the ambiguity plane approach and the Wigner–Ville time-frequency plane approach in terms of optimum cyclic-feature detection. Like the three conventional feature detectors (13), (15), and (17) considered in Section III, these two approaches are also ad hoc. They have not been derived from any objective design criterion. Nevertheless, we shall see that, when properly modified, they can be made equivalent to the optimum spectral-line-regeneration detector.

The ambiguity-plane approach to interception is to simply measure the symmetric ambiguity function

$$\rho_{x_t}(\tau, \nu) \triangleq \int_{-\infty}^{\infty} x_t(u+\tau/2)x_t(u-\tau/2)e^{i2\pi\nu u}\, du \tag{37}$$

[3] This MSK signal is an SQPSK signal with raised cosine carrier envelope.

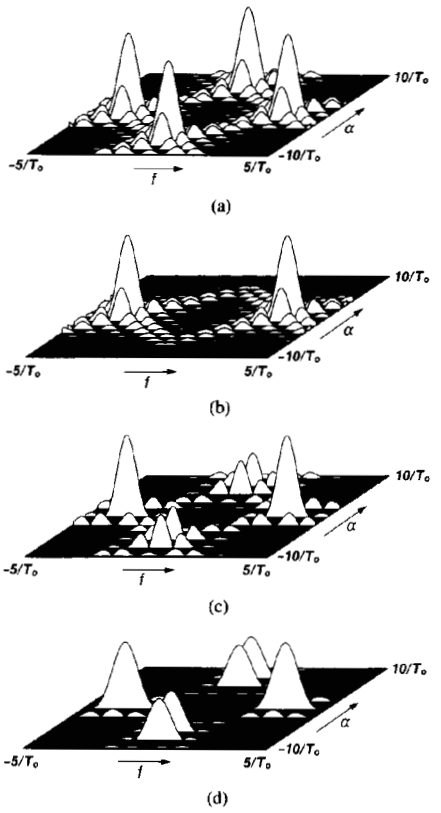

Fig. 2. Theoretical spectral correlation magnitudes for PSK signals with keying interval T_o and with full duty cycle rectangle envelopes and for MSK with half-cosine envelope. (a) BPSK. (b) QPSK. (c) SQPSK. (d) MSK.

for some sliding segment of $x(u)$, say

$$x_t(u) = \begin{cases} x(t+u), & |u| \leq T/2 \\ 0, & \text{otherwise,} \end{cases} \tag{38}$$

and then search for recognizable features in the ambiguity magnitude surface above the (τ, ν) plane as time t progresses. To relate this to the optimum detector in Section III, we observe that with (38) substituted into (37), we obtain by comparison to (24)

$$\frac{1}{T}\rho_{x_t}(\tau, \nu) = R_{x_T}^{-\nu}(t, \tau). \tag{39}$$

Thus, if the ambiguity function is correlated (over τ) with the ideal cyclic autocorrelation function for the signal of interest $s(t)$, as in (23), then we obtain the optimum detection statistic for a signal in white noise (down converted from frequency α to zero frequency by multiplication with $e^{-i2\pi\alpha t}$). Furthermore, since (26) and (39) reveal that the ambiguity function and the cyclic periodogram are a Fourier transform pair, then there is a close link between methods based on the ambiguity surface and those based on the unsmoothed cyclic periodogram surface. It should be clarified, however, that the ambiguity function (37) is not the familiar radar ambiguity function unless $x_t(u)$ is replaced with its complex envelope $\gamma_t(u)$, and the product $x_t(u + \tau/2)x_t(u - \tau/2)$ is replaced with $\gamma_t(u + \tau/2)\gamma_t^*(u - \tau/2)$ [23]. But, the ambiguity function for $x_t(u)$ cannot be recovered from the ambiguity function for $\gamma_t(u)$. The cross ambiguity based on $\gamma_t(u + \tau/2)\gamma_t(u - \tau/2)$ is needed as well. Thus, useful information that is present in the spectral correlation plane can be lost in the ambiguity plane if

the complex envelope γ_t is used in place of the real signal x_t. This is easy to see intuitively since the complex envelope discards all negative frequency components in the real signal, and therefore all spectral correlation between positive- and negative-frequency components is discarded. This is discussed in more detail in [7], [8], [14].

The Wigner–Ville time-frequency plane approach to interception is to simply measure the Wigner–Ville time-frequency function [24]

$$E_{x_t}(u, f) \triangleq \int_{-\infty}^{\infty} x_t(u+\tau/2)x_t(u-\tau/2)e^{-i2\pi f\tau}\, d\tau, \quad (40)$$

for some sliding segment of $x(u)$, say (38), and then to search for recognizable features in the magnitude surface above the (u, f) plane as time t progresses. To relate this to the ambiguity plane approach and to the optimum detector in Section III, we observe that the Wigner–Ville distribution and the ambiguity function are a double-Fourier transform pair

$$\rho_{x_t}(\tau, \nu) = \int_{-\infty}^{\infty}\int_{-\infty}^{\infty} E_{x_t}(u, f)e^{i2\pi(\nu u+\tau f)}\, du\, df. \quad (41)$$

Consequently, (26) and (39) reveal that

$$\frac{1}{T}E_{x_t}(u, f) = \int_{-\infty}^{\infty} S_{x_T}^{\alpha}(t, f)e^{i2\pi\alpha u}\, d\alpha. \quad (42)$$

Thus, the cyclic-periodogram and the Wigner–Ville distribution are a Fourier transform pair, and there is therefore a close link between methods based on the Wigner–Ville surface and those based on the unsmoothed cyclic periodogram. In order to render the Wigner–Ville time-frequency approach equivalent to the optimum detector in Section III, the Fourier transform of $E_{x_t}(\cdot, f)$ evaluated at α would have to be correlated with $S_s^{\alpha}(f)$ as in (25) (and the result upconverted from zero frequency to frequency α).

It is emphasized that the smoothing operation used in the spectral correlation plane (or cyclic-spectral analysis) method derived in Section IV from the optimum detector is important since the variance of the measured spectral correlation function is inversely proportional to the product of the collect time T and the smoothing window width Δf. (In fact, the SNR performance of the cyclic-spectral analysis detector (36) is proportional to $T\Delta f$ provided that Δf is not too large.) Thus, methods based directly on the Wigner–Ville distribution without smoothing in f would not be expected to perform comparably. Furthermore, the characteristic of the Wigner–Ville distribution, of adding contributions from *all* values of α as revealed by (42), is a probable source of poor performance for two reasons: 1), the signal of interest makes its primary contributions to the detection surface at only values of α equal to its cycle frequencies, and 2), even the contributions at the cycle frequencies of the signal should not in general be added directly without proper phase compensation. This is explained in the next section.

VI. Likelihood-Ratio Detection

To gain further insight into the potential and the limitations of the optimum spectral-line regeneration detector and its cyclic-spectral analysis adaptation, we shall uncover the relationship between the spectral-line regeneration detector and the likelihood-ratio detector. Specifically, it is well known that a monotonic function of the likelihood ratio, for a weak zero mean signal $s(t)$ in additive white Gaussian noise on the time interval $[t - T/2, t + T/2]$, is closely approximated by the quadratic form [25], [26]

$$y(t) = \frac{1}{N_o^2 T}\int_{-T/2}^{T/2}\int_{-T/2}^{T/2} R_s(t-u, t-v) \cdot x(t-u)x(t-v)\, du\, dv \quad (43)$$

where $R_s(u, v)$ is the signal autocorrelation function

$$R_s(u, v) = E\{s(u)s(v)\}. \quad (44)$$

Substitution of the representation (2) into (43) yields [7]

$$y(t) = \sum_{\alpha}\frac{1}{N_o^2}\int_{-T}^{T} R_s^{\alpha}(\tau)^* R_{x_T}^{\alpha}(t, \tau)\, d\tau \quad (45)$$

where $R_{x_T}^{\alpha}(t, \tau)$ is given by (24). Comparison of (45) to (23) reveals that this weak signal likelihood-ratio detector is simply the sum over all cycle frequencies of the complex envelopes of the maximum SNR spectral-line detection statistics,

$$y(t) = \sum_{\alpha} y_{\alpha}(t)e^{-i2\pi\alpha t} \quad (46)$$

where $y_{\alpha}(t)$ is given by (23). Thus, this *multicycle detector* generates all possible spectral lines at their maximum power level and then adds their complex envelopes together. Application of Parseval's relation to (45) [assuming that T exceeds an appropriate measure of the width of $R_s^{\alpha}(\tau)$] yields the alternative formula

$$y(t) = \sum_{\alpha}\frac{1}{N_o^2}\int_{-\infty}^{\infty} S_s^{\alpha}(f)^* S_{x_T}^{\alpha}(t, f)\, df. \quad (47)$$

Thus, this optimum multicycle detector measures the cyclic periodograms of the received corrupted signal $x(t)$ for all cycle frequencies α contained in the signal to be detected $s(t)$, correlates these (over f) with stored replicas of the ideal cyclic spectral densities of $s(t)$, and then adds up these correlations. If the signal were modeled as stationary, then only the $\alpha = 0$ term would remain and this would yield

$$y(t) = \frac{1}{N_o^2}\int_{-\infty}^{\infty} S_s^0(f)S_{x_T}^0(t, f)\, df, \quad (48)$$

which is the optimum radiometer (cf. [7]). If the only thing known about the signal $s(t)$ is its passband, say $[f_o - B/2, f_o + B/2]$, then (48) would be approximated by

$$y(t) = \frac{1}{N_o^2}\int_{f_o-B/2}^{f_o+B/2} S_{x_T}^0(t, f)\, df, \quad (49)$$

which is the standard radiometer.

If the additive noise plus interference is not white, but it is stationary and Gaussian, then the weak signal maximum-likelihood detector, (46) and (25), generalizes to (46) and (28), provided only that T is large enough that a spectral window of width $1/T$ will resolve $S_n^0(f)$. This can be verified using the standard noise-whitening approach to detection.

Unfortunately, even if the modulation type and its parameter values (e.g., carrier frequency and chip rate for a BPSK signal) are known, the optimum multicycle detector (47) cannot be implemented without knowledge of the phase of the signal because the quantities $S_s^{\alpha}(f)$ depend on this phase. For example, the spectral correlation function for $s'(t) = s(t - t_o)$ is

$$S_{s'}^{\alpha}(f) = S_s^{\alpha}(f)e^{-i2\pi\alpha t_o}. \quad (50)$$

Thus, if the wrong value for t_o is used, the resultant phases of the individual terms in (47) can result in destructive interference rather than constructive interference when the sum over α is performed.

Although (47) might not be practical for implementation, it lends further support to the cyclic spectral analysis approach to detection since this approach enables the user or an automated algorithm to exploit more than one cycle frequency of the signal of interest. This can be beneficial not only for detection,

but also for identification of signal-modulation type as well as for signal analysis (parameter estimation). In fact, it is shown in [13] that maximization of (47) with respect to signal parameters on which $S_s^\alpha(f)$ depends yields their weak signal maximum-likelihood estimates. Also, the alternative forms of implementation of maximum-likelihood detectors described in [21], which follow directly from (43) for the weak signal case, can possibly be more practical than (47) in some situations.

VII. Maximum-Deflection Detection

An alternative approach to arriving at the multicycle detector (47) as a detector with optimality properties is based on a performance measure called *deflection*. Specifically, the deflection is a measure of output SNR that is particularly appropriate for weak signal detection [26]–[27]. For a detection statistic $y(t)$, the deflection is defined by

$$d(t) \triangleq \frac{|E\{y(t)|s(t) \text{ present}\} - E\{y(t)|s(t) \text{ absent}\}|}{(\text{var}\{y(t)|s(t) \text{ absent}\})^{1/2}} \tag{51}$$

For a quadratic detector, we have the general representation

$$y(t) = \int_{-T/2}^{T/2} \int_{-T/2}^{T/2} k_t(u, v) x(t-u) x(t-v)\, du\, dv. \tag{52}$$

For the case in which $x(t)$ consists of either the signal $s(t)$ plus additive white Gaussian noise $n(t)$, $x(t) = s(t) + n(t)$, or just noise alone, $x(t) = n(t)$, substitution of (52) into (51) yields

$$d^2(t) = \frac{\left| \int_{-T/2}^{T/2} \int_{-T/2}^{T/2} k_t(u, v) R_s(t-u, t-v)\, du\, dv \right|^2}{2N_o^2 \int_{-T/2}^{T/2} \int_{-T/2}^{T/2} [k_t(u, v)]^2\, du\, dv} \tag{53}$$

[where it has been assumed without loss of generality that $k_t(u, v) = k_t(v, u)$]. Application of the Cauchy–Schwarz inequality to (53) yields the deflection-maximizing kernel [7]

$$k_t(u, v) = \frac{1}{N_o^2 T} R_s(t-u, t-v) \tag{54}$$

and the resultant maximum value of squared deflection

$$d^2(t)_{\max} = \frac{1}{2N_o^2} \int_{-T/2}^{T/2} \int_{-T/2}^{T/2} [R_s(t-u, t-v)]^2\, du\, dv. \tag{55}$$

It follows from (52) and (54) that the quadratic detector that maximizes deflection is identical to the weak signal likelihood-ratio detector (43), which is a multicycle detector (47). Furthermore, the value of maximized deflection is completely characterized by the maximized SNR's (21) obtained from the optimum single-cycle detectors (25). Specifically, substitution of (2) into (55) yields

$$d^2(t)_{\max} = \frac{1}{2N_o^2} \sum_{\alpha,\beta} \int_{-T}^{T} R_s^\alpha(\tau) R_s^\beta(\tau) \cdot \frac{\sin[\pi(\alpha+\beta)(T-|\tau|)]}{\pi(\alpha+\beta)} d\tau e^{-i2\pi(\alpha+\beta)t} \tag{56}$$

$$\cong \frac{T}{2N_o^2} \sum_{\alpha} \int_{-T}^{T} |R_s^\alpha(\tau)|^2\, d\tau \tag{57}$$

$$\cong \frac{T}{2N_o^2} \sum_{\alpha} \int_{-\infty}^{\infty} |S_s^\alpha(f)|^2\, df. \tag{58}$$

The approximation (57) is accurate if T is sufficiently large relative to the longest period of cyclostationarity ($T \gg 1/\alpha_{\min}$), and sufficiently large relative to the largest width of the cyclic autocorrelations $R_s^\alpha(\tau)$. The latter condition on T also renders (58) a close approximation. Comparison of (58) to (21) (including $\alpha = 0$) for the case of white noise ($S_n^0(f) = N_o$) yields the characterization

$$d^2(t)_{\max} \cong \sum_{\alpha} \text{SNR}_{\max}^\alpha. \tag{59}$$

The preceding equivalence between the maximum-deflection quadratic detector and the weak signal likelihood-ratio detector holds as well for nonwhite stationary Gaussian noise (e.g., interference plus noise), and the performance characterization (59) also holds with SNR^α given by (21) (including $\alpha = 0$).

In addition to this reinterpretation of the weak signal likelihood-ratio detector (the multicycle detector), we can also reinterpret the maximum-SNR single-cycle detector as a maximum-deflection detector. Specifically, it can be shown that when a detector includes a narrow bandpass filter with center frequency α at its output, then

$$\text{SNR}^\alpha \cong d_\alpha^2(t) \quad \alpha \neq 0 \tag{60}$$

where d_α is the deflection (51) for this detector with output $y_\alpha(t)$.

VIII. A Fundamental Distinction Between Radiometers and Cycle Detectors

The fact that (21) and therefore (60) are valid only for $\alpha \neq 0$ is at the heart of the difference between the radiometer (48) and the cycle detector (25). The reason that (21) is not valid for $\alpha = 0$ is that the radiometer output contains a spectral line at $\alpha = 0$ regardless of whether or not the signal is present, whereas the cycle detector contains a spectral line at $\alpha \neq 0$ only if the signal is present. Thus, the radiometer must distinguish between the strength of the spectral line at $\alpha = 0$ due to signal plus noise and/or interference, and the spectral line at $\alpha = 0$ due only to noise and/or interference, whereas the cycle detector need only distinguish between the presence and absence of a spectral line at $\alpha \neq 0$. This follows directly from the formula [8], [13]

$$P_y^\alpha = \left| \int_{-\infty}^{\infty} K(f + \alpha/2, f - \alpha/2) S_x^\alpha(f)\, df \right|^2 \tag{61}$$

for the spectral-line power of any quadratic detector [K is the double Fourier transform of the kernel k, cf. (19)], and the fact that

$$S_x^\alpha(f) = \begin{cases} S_s^\alpha(f), & \alpha \neq 0, \text{ signal present} \\ S_s^0(f) + S_n^0(f), & \alpha = 0, \text{ signal present} \\ 0 & \alpha \neq 0, \text{ signal absent} \\ S_n^0(f), & \alpha = 0, \text{ signal absent} \end{cases} \tag{62}$$

where it is assumed that the noise plus interference $n(t)$ does not exhibit cyclostationarity with cycle frequency α, $S_n^\alpha(f) \equiv 0$. This fact also results in the following differences in the asymptotic behavior of the detection statistics for the optimum radiometer [(25) with $\alpha = 0$] and the optimum cycle detector [(25) with $\alpha \neq 0$]:

$$\lim_{T \to \infty} |y_\alpha(t)| = \begin{cases} \dfrac{1}{N_o^2} \displaystyle\int_{-\infty}^{\infty} |S_s^\alpha(f)|^2\, df, \\ \qquad \alpha \neq 0, \text{ signal present} \\ 0, \quad \alpha \neq 0, \text{ signal absent} \end{cases} \tag{63}$$

$$\lim_{T\to\infty} |y_\alpha(t)| = \begin{cases} \dfrac{1}{N_o^2}\displaystyle\int_{-\infty}^{\infty} S_s^0(f)[S_s^0(f)+S_n(f)]\ df, \\ \qquad \alpha = 0, \quad \text{signal present} \\ \dfrac{1}{N_o^2}\displaystyle\int_{-\infty}^{\infty} S_s^0(f)S_n^0(f)\ df, \\ \qquad \alpha = 0, \quad \text{signal absent.} \end{cases} \tag{64}$$

A measure of performance that is comparable to SNR^α for the radiometer ($\alpha = 0$) can be obtained as follows. The strength of the spectral line at $\alpha = 0$ regenerated by any quadratic detector with kernel $k_0(u, v)$ [cf. (12)] is given by [8]

$$P_y^0 = \left[\int_{-\infty}^{\infty} S_x^0(f)K_0(f, f)\ df\right]^2. \tag{65}$$

If the signal is present, then $S_x^0(f) = S_s^0(f) + S_n^0(f)$. Otherwise, $S_x^0(f) = S_n^0(f)$. If the noise-plus-interference spectral-line power

$$P_{y|n}^0 = \left[\int_{-\infty}^{\infty} S_n^0(f)K_0(f, f)\ df\right]^2 \tag{66}$$

is known, then its effect can be subtracted from the detector output, and we can thus define SNR^0 to be the ratio of the spectral line power due only to the signal, to the power of the output noise-plus-interference that is continuously distributed versus frequency throughout the band of width $1/T$ centered at $f = 0$. The resultant formula for SNR^0 would then be given by (21) with $\alpha = 0$. Furthermore, if the detector includes a low-pass filter at its output, then the deflection characterization (60) would be valid with $\alpha = 0$. But it must be emphasized that the preceding justification for use of the conventional deflection performance-measure [(21) and (60) with $\alpha = 0$] is predicated on the assumption that the spectral-line power (66) due to noise plus interference is *known*. When it is not known and, worse yet, changes with time, the deflection is not an appropriate measure of the performance of the radiometer. Moreover, in this case, the radiometer unlike the cycle detector is faced with the difficult task of detecting the presence of the signal spectral-line power

$$P_{y|s}^0 = \left[\int_{-\infty}^{\infty} S_s^0(f)K_0(f, f)\ df\right]^2 \tag{67}$$

which is superimposed on the possibly much larger unknown and changing-noise-plus-interference spectral-line power (66). This greatly complicates the problem of setting the threshold level to be used with the radiometer, and renders the radiometric approach to detection inherently more susceptible to unknown and/or changing noise and interference, especially for weak signals. This is corroborated by performance comparisons to cycle detectors to be reported in a sequel to this paper. The following example demonstrates the superiority of cycle detectors for a BPSK signal in a variable white noise background.

Example: Let us consider a BPSK signal, with keying interval T_o and carrier frequency f_c, to be detected in the presence of white Gaussian noise with a mean spectral density level $E\{N_o\}$ that results in an in-band SNR of 0 dB (i.e., the expected noise power within the signal band $B = \{f: |f + f_c| \leq 2/T_o\}$ is equal to the expected signal power). The spectral density level N_o is a positive-valued random variable from which a statistically independent random sample is drawn for each collection interval. Its coefficient of variation is equal to 1/10,

$$\frac{\text{var}\{N_o\}}{(E\{N_o\})^2} = \frac{1}{10}.$$

The collection time T contains 128 keying intervals, each of which contains 16 time samples. The receiver operating characteristics for three detectors were determined from simulations and are shown in Fig. 3. It can be seen that the optimum cycle detector corresponding to $\alpha = 2f_c$ performs the best, the optimum cycle detector corresponding to $\alpha = 1/T_o$ performs next best, and the optimum radiometer performs the worst. The relative performances of the two cycle detectors is consistent with the relative strengths of their features as shown in Fig. 2(a).

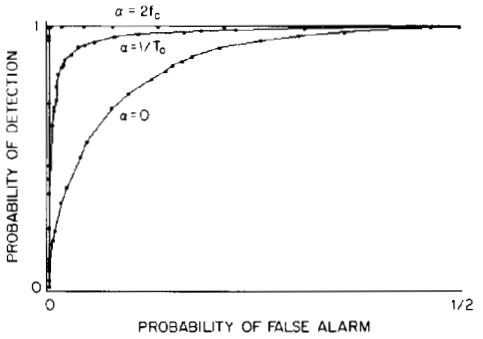

Fig. 3. Receiver operating characteristics for three detectors for a simulated BPSK signal in white Gaussian noise with random spectral density level having a coefficient of variation of 1/10.

IX. Conclusions

In this paper, a unifying approach to the design and analysis of quadratic detectors for signal interception is presented. The methods of detection that are incorporated in this unification include radiometry, delay-and-multiply chip-rate feature detection, filter-and-square carrier feature detection, dual-channel correlation detection, ambiguity-plane feature detection, Wigner–Ville time-frequency plane feature detection, spectral-correlation plane feature detection, likelihood-ratio detection for weak signals, maximum-deflection detection, and optimum spectral-line regeneration detection. The unification reveals the fundamental role that spectral correlation and spectral-line regeneration play in the signal interception problem, and shows how to modify various ad hoc techniques to make them optimum. It also suggests the spectral-correlation plane approach as a general approach to interception that offers great flexibility as well as inherent tolerance to one of the most challenging problems in interception, namely, accommodating unknown and changing noise level and interference activity. This tolerance is illustrated in an example involving the detection of a BPSK signal in a variable white noise background.

Acknowledgment

The author expresses his gratitude to C. M. Spooner for performing the simulations briefly described in the example in Section VIII.

References

[1] H. Urkowitz, "Energy detection of unknown deterministic signals," *Proc. IEEE*, vol. 55, pp. 523–531, 1967.

[2] R. A. Dillard, "Detectability of spread-spectrum signals," *IEEE Trans. Aerosp. Electron. Syst.*, vol. AES-15, pp. 526–537, 1979.

[3] D. G. Woodring, "Performance of optimum and suboptimum detectors for spread spectrum waveforms," Naval Research Lab., Washington, D.C., Rep. 8432, Dec. 1980.

[4] M. K. Simon, J. K. Omura, R. A. Scholtz, and B. K. Levitt, *Spread Spectrum Communications, Vol. III.* Rockville, MD: Computer Science, 1985, pt. 5, ch. 4.
[5] D. J. Torrieri, *Principles of Secure Communication Systems.* Dedham, MA: Artech, 1985.
[6] F. Amoroso, "Energy detection with uncertain system temperature," in *Proc. MILCOM 1982,* Bedford, MA, Oct. 17–20, 1982, pp. 19.4-1–19.4-5.
[7] W. A. Gardner, *Introduction to Random Processes with Applications to Signals and Systems.* New York: Macmillan, 1985.
[8] ——, *Statistical Spectral Analysis: A Nonprobabilistic Theory.* Englewood Cliffs, NJ: Prentice-Hall, 1987.
[9] R. O. Schmidt, "Multiple emitter location and signal parameter estimation," presented at Proc. RADC Spectrum Estimation Workshop, Oct. 3–5, 1979.
[10] K. D. Snow, J. Rogers, and D. R. Hui, "Principles of spread spectrum interception," Probe Systems, Inc., Sunnyvale, CA, PSI-DC-754 or PSI-ER-5149-05, Feb. 1978 (classified).
[11] P. J. Munday and M. C. Pinches, "Jaguar-V frequency-hopping radio system," *Proc. IEE,* vol. 129, Pt. F, pp. 213–222, June 1982.
[12] W. A. Gardner, "Measurement of spectral correlation," *IEEE Trans. Acoust., Speech, Signal Processing,* vol. ASSP-34, pp. 1111–1123, Oct. 1986.
[13] ——, "The role of spectral correlation in design and performance analysis of synchronizers," *IEEE Trans. Commun.,* vol. COM-34, pp. 1089–1095, Nov. 1986.
[14] ——, "The spectral correlation theory of cyclostationary time-series," *Signal Processing,* vol. 11, pp. 13–36, July 1986.
[15] ——, "Spectral correlation of modulated signals, Part I—Analog modulation," *IEEE Trans. Commun.,* vol. COM-35, pp. 584–594, June 1987.
[16] W. A. Gardner, W. A. Brown, and C.-K. Chen, "Spectral correlation of modulated signals, Part II—Digital modulation," *IEEE Trans. Commun.,* vol. COM-35, pp. 595–601, June 1987.
[17] R. A. Boyles and W. A. Gardner, "Cycloergodic properties of discrete-parameter nonstationary stochastic processes," *IEEE Trans. Inform. Theory,* vol. IT-29, pp. 105–114, Jan. 1983.
[18] W. A. Gardner, "Stationarizable random processes," *IEEE Trans. Inform. Theory,* vol. IT-24, pp. 8–22, Jan. 1978.
[19] L. E. Franks, "Carrier and bit synchronization in data communication—A tutorial review," *IEEE Trans. Commun.,* vol. COM-28, pp. 1107–1121, 1980.
[20] R. E. Ziemer and R. L. Peterson, *Digital Communications and Spread Spectrum Systems.* New York: Macmillan, 1985.
[21] N. F. Krasner, "Optimal detection of digitally modulated signals," *IEEE Trans. Commun.,* vol. COM-30, pp. 885–895, 1982.
[22] G. M. Jenkins and D. G. Watts, *Spectral Analysis and its Applications.* San Francisco, CA: Holden-Day, 1968.
[23] A. W. Rihaczek, *Principles of High-Resolution Radar.* New York: McGraw-Hill, 1969.
[24] T. A. C. M. Claasen, and W. F. G. Mecklenbrauker, "The Wigner distribution—A tool for time-frequency signal analysis, Parts I-III, *Phil. J. Res.,* vol. 35, pp. 217–250, 276–300, 372–389, 1980.
[25] W. A. Gardner, "Structural characterization of locally optimum detectors in terms of locally optimum estimators and correlators," *IEEE Trans. Inform. Theory,* vol. IT-28, pp. 924–932, Nov. 1982.
[26] H. L. Van Trees, *Detection, Estimation, and Modulation Theory, Part III.* New York: Wiley, 1971.
[27] W. A. Gardner, "A unifying view of second-order measures of quality for signal classification," *IEEE Trans. Commun.,* vol. COM-28, pp. 807–816, June 1980.

★

William A. Gardner (S'64–M'67–SM'84) was born in Palo Alto, CA, on November 4, 1942. He received the M.S. degree from Stanford University, Stanford, CA, in 1967, and the Ph.D. degree from the University of Massachusetts, Amherst, in 1972, both in electrical engineering.

He was a Member of the Technical Staff at Bell Laboratories in Massachusetts from 1967 to 1969. He has been a faculty member at the University of California, Davis, since 1972, where he is a Professor of Electrical Engineering and Computer Science. His research interests are in the general area of statistical signal processing, with primary emphasis on the theories of time-series analysis, stochastic processes, and signal detection and estimation.

Dr. Gardner is the author of *Introduction to Random Processes with Applications to Signals and Systems*, Macmillan, 1985, and *Statistical Spectral Analysis: A Nonprobabilistic Theory*, Prentice-Hall, 1987. He holds several patents and is the author of over 50 research-journal papers. He received the 1987 Distinguished Engineering Alumnus Award from the University of Massachusetts. He is a member of the American Mathematical Society, the Mathematical Association of America, the American Association for the Advancement of Science, and the European Association for Signal Processing.